Expanded View Figures

Figure EV1. Rescuing effect of ectopically expressed CNOT6L in *Cnot6l*$^{-/-}$ oocytes.

A Gene targeting strategy for CRISPR/Cas9-based mouse *Cnot6l* knockout. F, forward; R, reverse; Stop, stop codon; gRNA, guide RNA.

B PCR results using tail genomic DNA as the template. The WT allele ("+") and 10-nucleotide-deletion allele ("−") were amplified with the primer pairs GT-F1, GT-F2, and GT-R. Primer sequences were provided in Appendix Table S1.

C, D Western blot of CNOT6 and CNOT6L in HeLa cells transfected with plasmids expressing Flag-CNOT6 or Flag-CNOT6L (C) and in oocytes (WT and *Cnot6l* null) at the MI stage (D).

E A diagram showing the major functioning domains of mouse CNOT6L protein.

F–H Rates of PB1 emission (F), representative images and immunofluorescent staining of α-tubulin (G), and rates of normal spindle assembly (H) in oocytes cultured for 16 h. Arrows indicate polar body-1 (PB1). Fully grown GV oocytes were microinjected with mRNAs encoding CNOT6L, CNOT6L$^{\Delta LRR}$, or CNOT6L^{E235A} and were released from meiotic arrest at 12 h after microinjection. Rescue: oocytes contain normal shaped bipolar spindle and aligned chromosomes; partial rescue: oocytes contain normal shaped bipolar spindle but chromosomes were not properly aligned; abnormal: both spindle assembly and chromosome alignment failed in oocytes. Scale bar, 20 μm. Error bars, SEM. *$P < 0.05$; **$P < 0.01$; ***$P < 0.001$ by two-tailed Student's *t*-test. n.s.: non-significant. The numbers of analyzed oocytes are indicated (*n*) in (H). $n = 3$ biological replicates in (F).

I Co-IP results showing interactions of CNOT6L, CNOT6L^{E235A}, and CNOT6L$^{\Delta LRR}$ with CNOT7. HeLa cells were co-transfected with plasmids expressing HA-CNOT6L and FLAG-CNOT7 for 48 h before immunoprecipitation.

Source data are available online for this figure.

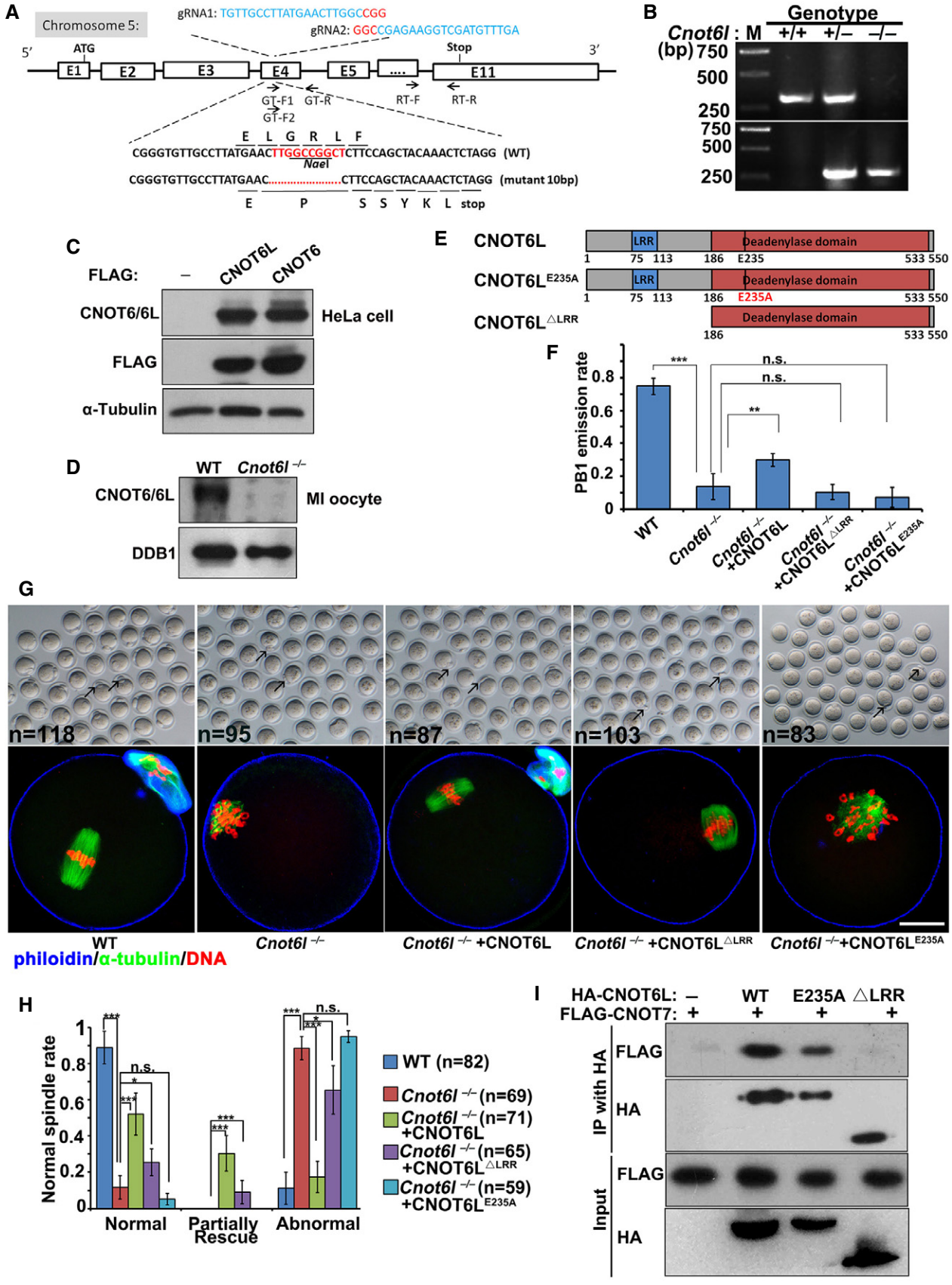
A
Chromosome 5:
gRNA1: TGTTGCCTTATGAACTTGGCCGG
gRNA2: GGCCGAGAAGGTCGATGTTTGA
5′
ATG
E1
E2
E3
E4
E5
....
Stop
E11
3′
GT-F1
GT-F2
GT-R
RT-F
RT-R
E L G R L F
CGGGTGTTGCCTTATGAACTTGGCCGGCTCTTCCAGCTACAAACTCTAGG (WT)
NaeI
CGGGTGTTGCCTTATGAAC.....CTTCCAGCTACAAACTCTAGG (mutant 10bp)
E P S S Y K L stop
B
Genotype
Cnot6l : M +/+ +/– –/–
(bp) 750
500
250
750
500
250
C
FLAG: – CNOT6L CNOT6
CNOT6/6L
FLAG
α-Tubulin
HeLa cell
D
WT Cnot6l −/−
CNOT6/6L
DDB1
MI oocyte
E
CNOT6L
CNOT6L E235A
CNOT6L △LRR
LRR
Deadenylase domain
1 75 113 186 E235 533 550
E235A
F
PB1 emission rate
0 0.2 0.4 0.6 0.8
***
n.s.
n.s.
**
WT
Cnot6l −/−
Cnot6l −/− +CNOT6L
Cnot6l −/− △LRR +CNOT6L
Cnot6l −/− +CNOT6L E235A
G
n=118
n=95
n=87
n=103
n=83
WT
Cnot6l −/−
Cnot6l −/− +CNOT6L
Cnot6l −/− +CNOT6L△LRR
Cnot6l −/− +CNOT6L E235A
philoidin/α-tubulin/DNA
H
Normal spindle rate
0 0.2 0.4 0.6 0.8 1
***
n.s.
*
***
***
***
***
n.s.
Normal
Partially Rescue
Abnormal
WT (n=82)
Cnot6l −/− (n=69)
Cnot6l −/− (n=71) +CNOT6L
Cnot6l −/− (n=65) +CNOT6L△LRR
Cnot6l −/− (n=59) +CNOT6L E235A
I
HA-CNOT6L: – WT E235A △LRR
FLAG-CNOT7: + + + +
IP with HA
FLAG
HA
Input
FLAG
HA

Figure EV1.

Figure EV2. Phenotypic analyses of *Cnot6l*$^{-/-}$ female mice.

A Hematoxylin and eosin staining showing ovarian histology of WT and *Cnot6l*$^{-/-}$ mice. Scale bar, 100 μm.

B, C Representative images (B) and numbers (C) of cumulus–oocyte complexes (COCs) and denuded oocytes collected from antral follicles of WT and *Cnot6l*$^{-/-}$ mice. Scale bar, 100 μm. Error bars, SEM. n.s.: non-significant. The numbers of analyzed mice are indicated (*n*).

D Percentage (%) of oocytes containing a surrounded nucleolus (SN) among oocytes in (B). Error bars, SEM. n.s.: non-significant. The numbers of analyzed mice are indicated (*n*).

E Confocal microscopy results showing representative oocytes containing a non-surrounded nucleolus (NSN) or a surrounded nucleolus (SN) among oocytes in (B). Percentages of NSN and SN oocytes among the total oocytes being collected are indicated in the corner. Scale bar, 20 μm.

F Representative images of zygotes collected from oviducts of WT and *Cnot6l*$^{-/-}$ female mice at 24 h after hCG injection and were mated with WT male mice. Scale bar, 100 μm.

G Confocal microscopy results showing representative zygotes containing 2 or 3 pronuclei. Scale bar, 20 μm.

H Quantification of pronucleus formation rates in zygotes shown in (F). Error bars, SEM. n.s.: non-significant. The numbers of analyzed zygotes are indicated (*n*).

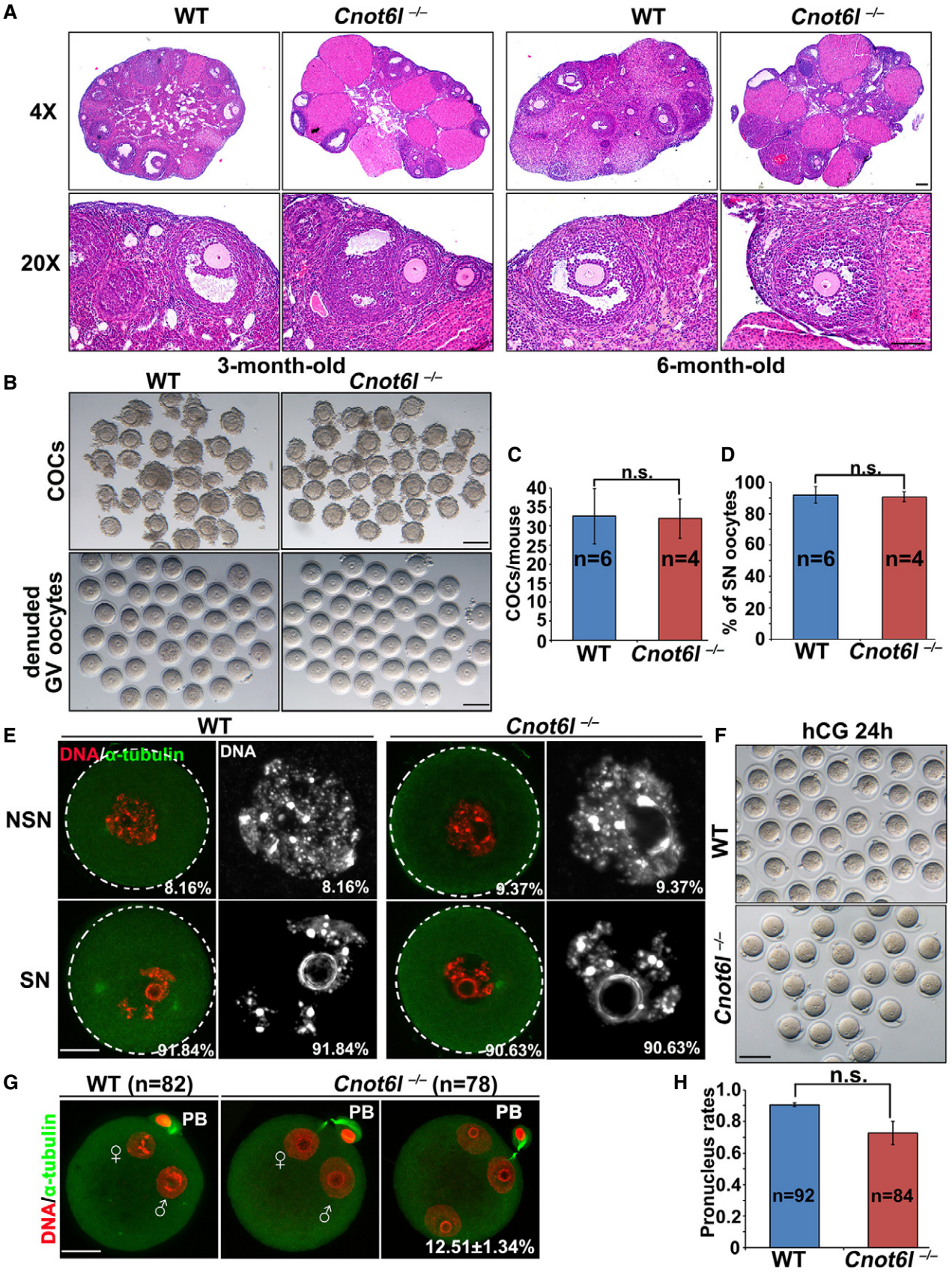

Figure EV2.

Figure EV3. RNA sequencing analyses of oocytes and zygotes derived from WT, *Cnot6l*$^{-/-}$, and *Btg4*$^{-/-}$ female mice.

A Heatmap of Spearman correlation coefficients of total transcripts among WT, *Cnot6l*$^{-/-}$, and *Btg4*$^{-/-}$ oocytes and embryos at different stages.

B Global mRNA levels in WT, *Cnot6l*$^{-/-}$, and *Btg4*$^{-/-}$ oocytes at different stages. The expression level of each transcript is normalized by mRNA encoding mCherry, which was *in vitro* transcribed and equally added to each sample before RNA extraction. The box indicates upper and lower quantiles, the thick line in the box indicates the median, and the whiskers represent 2.5th and 97.5th percentiles. ***$P < 0.001$ by two-tailed Student's *t*-test.

C Scatter plot comparing transcripts between WT and *Cnot6l*$^{-/-}$ oocytes (at GV, MI, and MII stages) and zygotes derived from these oocytes. Transcripts decreased or increased more than 2-fold in *Cnot6l*$^{-/-}$ oocyte samples were highlighted with blue or red, respectively.

D Number of genes up- and downregulated during GV-to-MII transitions.

E, F Gene ontology analysis of transcripts significantly degraded during GV-to-MII transition (GV/MII > 10) in WT oocytes but were stabilized in *Cnot6l*$^{-/-}$ (E) or *Btg4*$^{-/-}$ oocytes (F).

G RNA-seq results showing the relative expression levels (MII/GV) of representative transcripts in WT, *Cnot6l*$^{-/-}$, and *Btg4*$^{-/-}$ oocytes.

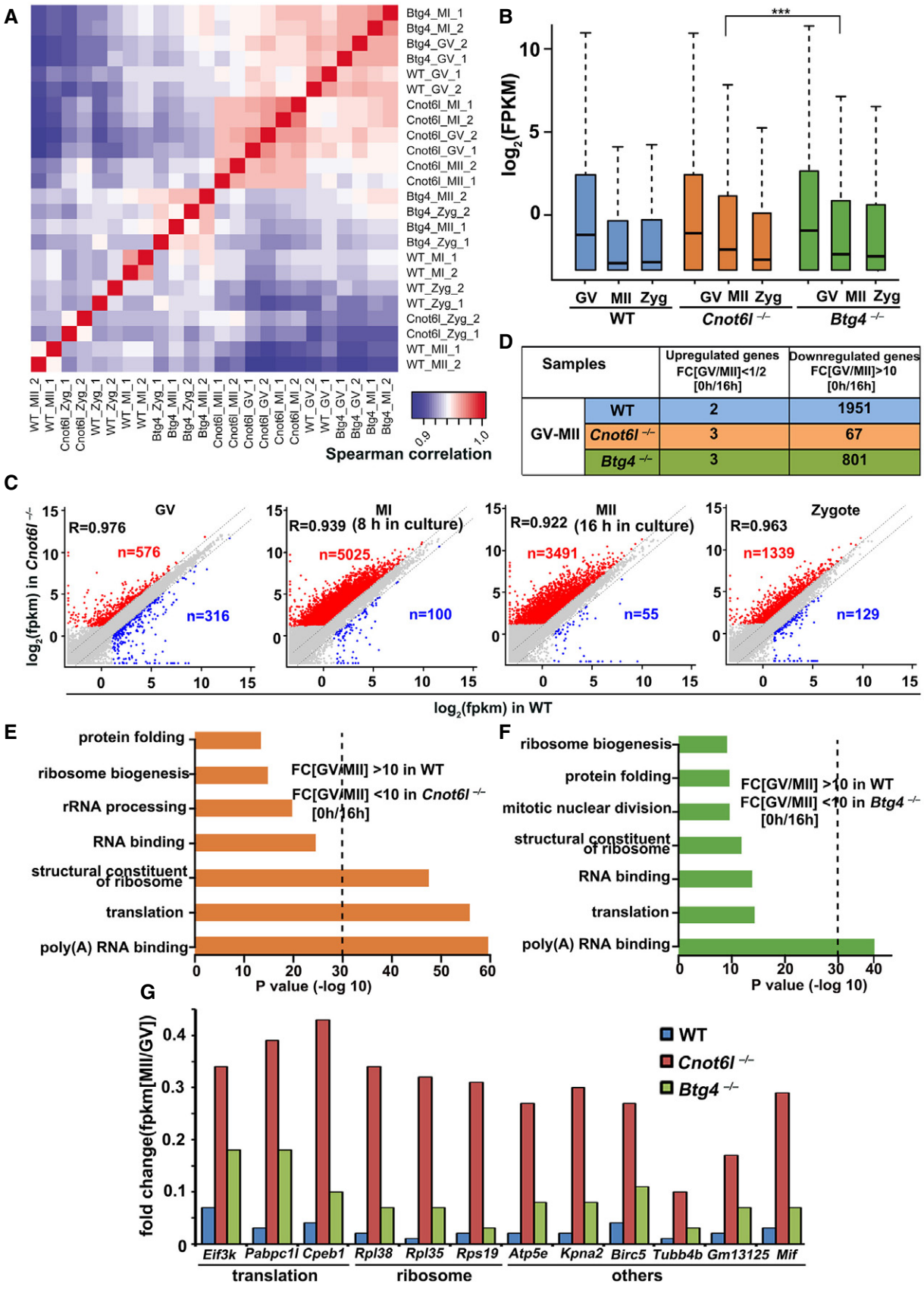
A
Btg4_MI_1
Btg4_MI_2
Btg4_GV_2
Btg4_GV_1
WT_GV_1
WT_GV_2
Cnot6l_MI_1
Cnot6l_MI_2
Cnot6l_GV_2
Cnot6l_GV_1
Cnot6l_MII_2
Cnot6l_MII_1
Btg4_MII_2
Btg4_Zyg_2
Btg4_MII_1
Btg4_Zyg_1
WT_MI_1
WT_MI_2
WT_Zyg_2
WT_Zyg_1
Cnot6l_Zyg_2
Cnot6l_Zyg_1
WT_MII_1
WT_MII_2
0.9
1.0
Spearman correlation
B
***
log2(FPKM)
10
5
0
GV MII Zyg
GV MII Zyg
GV MII Zyg
WT
Cnot6l −/−
Btg4 −/−
D
Samples
Upregulated genes FC[GV/MII]<1/2 [0h/16h]
Downregulated genes FC[GV/MII]>10 [0h/16h]
GV-MII
WT 2 1951
Cnot6l −/− 3 67
Btg4 −/− 3 801
C
GV
R=0.976
n=576
n=316
MI
R=0.939 (8 h in culture)
n=5025
n=100
MII
R=0.922 (16 h in culture)
n=3491
n=55
Zygote
R=0.963
n=1339
n=129
log2(fpkm) in Cnot6l −/−
log2(fpkm) in WT
E
protein folding
ribosome biogenesis
rRNA processing
RNA binding
structural constituent of ribosome
translation
poly(A) RNA binding
FC[GV/MII] >10 in WT
FC[GV/MII] <10 in Cnot6l −/−
[0h/16h]
P value (-log 10)
F
ribosome biogenesis
protein folding
mitotic nuclear division
structural constituent of ribosome
RNA binding
translation
poly(A) RNA binding
FC[GV/MII] >10 in WT
FC[GV/MII] <10 in Btg4 −/−
[0h/16h]
P value (-log 10)
G
fold change(fpkm[MII/GV])
0.4
0.3
0.2
0.1
0
WT
Cnot6l −/−
Btg4 −/−
Eif3k Pabpc1l Cpeb1 Rpl38 Rpl35 Rps19 Atp5e Kpna2 Birc5 Tubb4b Gm13125 Mif
translation
ribosome
others

Figure EV3.

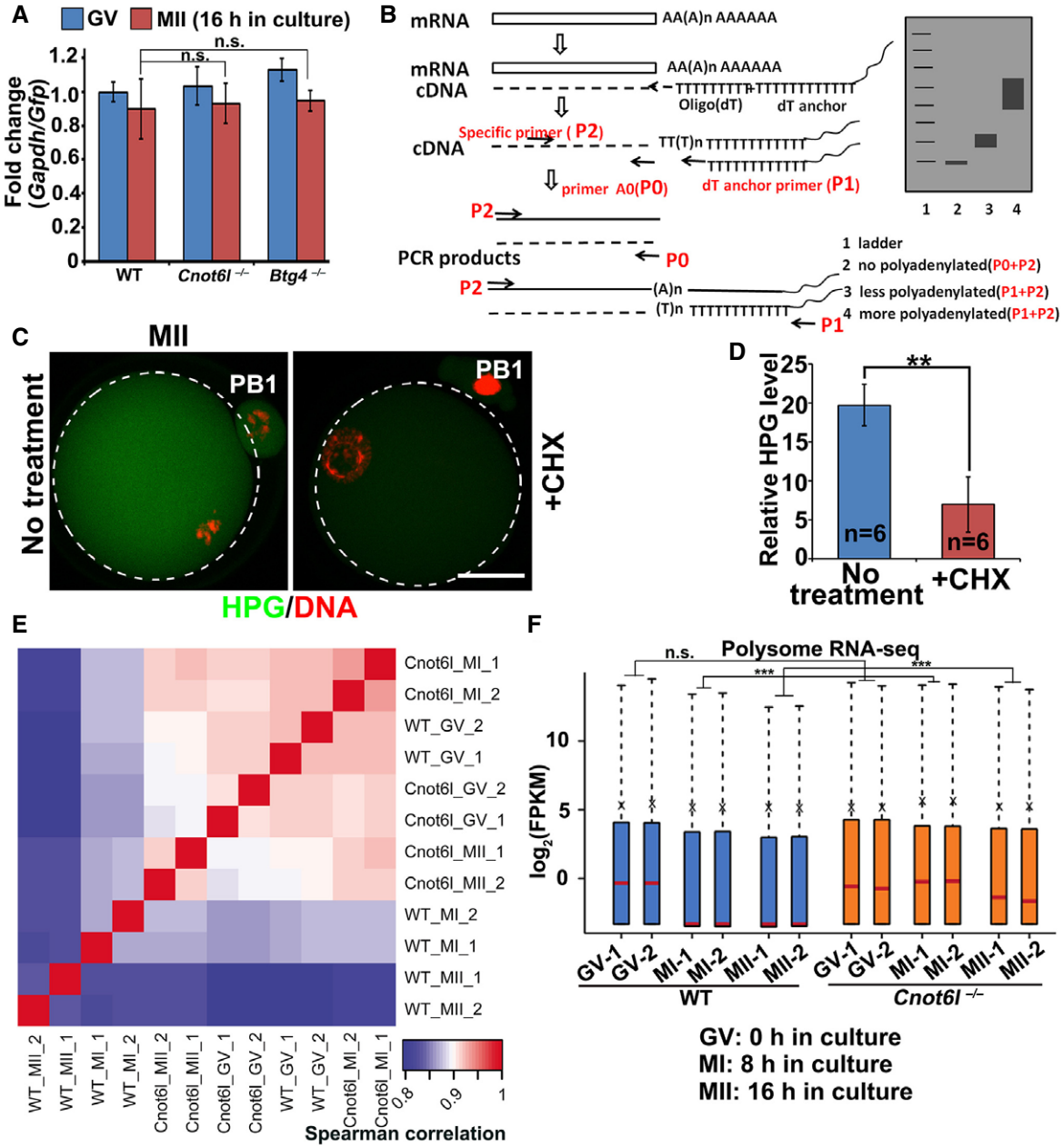

Figure EV4. Transcriptome analyses of maturing oocytes derived from WT and *Cnot6l*$^{-/-}$ mice.

A Quantitative RT–PCR (qRT–PCR) showing the relative levels between *Gapdh* and *Gfp* in GV and MII oocytes collected from WT, *Cnot6l*$^{-/-}$, and *Btg4*$^{-/-}$ mice. mRNAs encoding GFP were *in vitro* transcribed and equally added to each sample (0.1 ng/μl) before RNA extraction. Error bars, SEM. n.s.: non-significant. n = 3 technical replicates.

B Strategy of the mRNA poly(A) tail assay. P0, primer A0 that located at the end of mRNA 3′TUR without poly (A); P1, dT anchor primer (GCGAGCTCCGCGGCCGCGT12); P2, gene-specific primer.

C, D Immunofluorescence (C) and quantification (D) of HPG showing the overall translation levels of MII oocytes cultured in medium with or without cycloheximide (CHX, 20 μM). Scale bar, 20 μm. $^{**}P < 0.01$ by two-tailed Student's t-test. n = 3 biological replicates.

E Heatmap of Spearman correlation coefficients of transcripts associated with polysomes in WT and *Cnot6l*$^{-/-}$ oocytes at GV, MI, and MII stages.

F Levels of polysome-bound transcripts in WT and *Cnot6l*$^{-/-}$ oocytes at indicated stages (two biological repeats). The expression level of each transcript was normalized by the mCherry spike-in, which was *in vitro* transcribed and equally added to each sample before RNA extraction. The box indicates upper and lower quantiles, the red line in the box indicates the median, and the whiskers represent 2.5th and 97.5th percentiles, respectively. $^{***}P < 0.001$ by two-tailed Student's t-test. n.s.: non-significant.

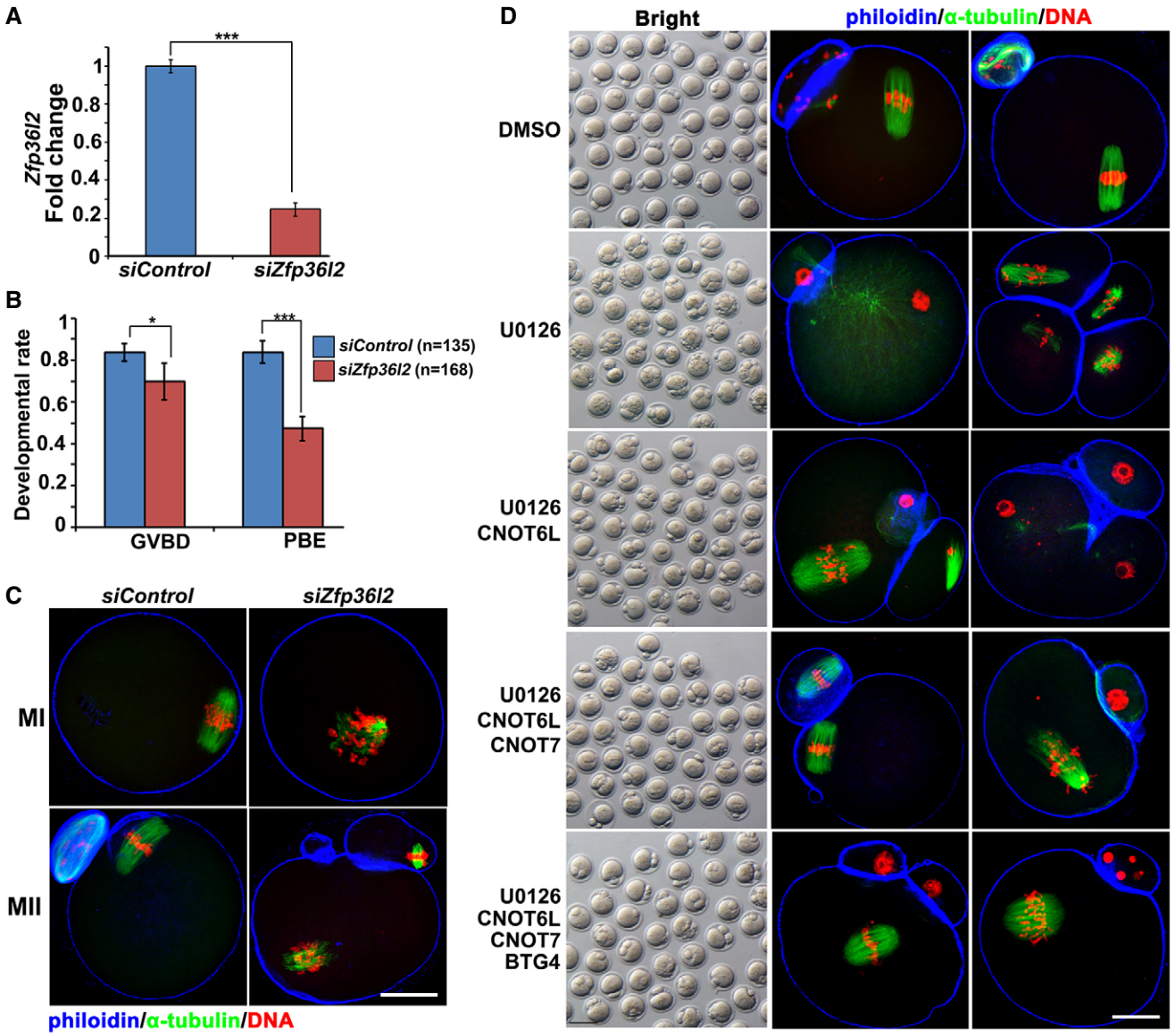

Figure EV5. Role of *Zfp36l2* and ERK1/2 in regulating meiotic maturation of mouse oocyte.

A qRT–PCR results showing the efficiency of *Zfp36l2* RNA interference in oocytes at the GV stage. $n = 3$ technical replicates. Error bars, SEM. ***$P < 0.001$ by two-tailed Student's *t*-test.

B GVBD and PB1 emission rates of oocytes microinjected control and *Zfp36l2*-targeted siRNAs. Error bars, SEM. *$P < 0.05$; ***$P < 0.001$ by two-tailed Student's *t*-test. The numbers of analyzed oocytes are indicated (*n*).

C Confocal microscopy results showing spindle assembly at MI and MII stages in oocytes microinjected with control siRNAs or *siZfp36l2*. Scale bar, 20 μm.

D PB2 emission and spindle assembly in oocytes cultured with or without U0126 treatment. Fully grown GV oocytes were microinjected with mRNAs encoding CNOT6L, CNOT7, and/or BTG4 and are released from milrinone at 12 h after microinjection. Then, the oocytes were further culture for 24 h with or without adding U0126 (20 μM) to the medium. Scale bar, 100 μm in brightfield images; Scale bar, 20 μm in immunofluorescence staining images.